

## A COMPARATIVE ANALYSIS OF TURBULENCE MODELS APPLIED TO COMPLEX FLOW

**Daniel A. Salinas Casanova** – salinas@unioeste.br

Universidade Estadual do Oeste do Paraná, Centro de Engenharias e Ciências Exatas  
85.855-000, Foz do Iguaçu, PR, Brasil

**César J. Deschamps** – deschamps@nrva.ufsc.br

**Alvaro T. Prata** – prata@nrva.ufsc.br

**Francisco F. S. Matos** – fred@nrva.ufsc.br

Universidade Federal de Santa Catarina, Departamento de Engenharia Mecânica  
80.040-900 – Florianópolis, SC, Brasil

**Abstract.** *The work is a comparative analysis of two  $k$ - $\epsilon$  turbulence models applied to a flow under the combined effects of stagnation, streamline curvature, stiff pressure gradient and recirculation. For such flow situations, it has been found that standard versions of  $k$ - $\epsilon$  model fail to predict even the most basic flow features unveiled by experimental data. Recently, a new version of  $k$ - $\epsilon$  model, developed from Renormalization Group (RNG) theory, has been proposed and successfully applied to a number of flows where other  $k$ - $\epsilon$  models have shown poor results. The reason for this superior performance of the RNG  $k$ - $\epsilon$  model cannot be easily explained since most works in the literature focus their attention only on results for quantities associated to the mean velocity field, without any reference to turbulence quantities. In the present investigation, the RNG  $k$ - $\epsilon$  model is compared to the widely used Launder & Sharma's  $k$ - $\epsilon$  model in the prediction of a complex flow. An assessment of the superior results found with the RNG  $k$ - $\epsilon$  model is provided through results for eddy viscosity and turbulence length scale.*

**Keywords:** *Renormalization Group (RNG) theory, Eddy viscosity models, Turbulence modeling*

### 1. INTRODUCTION

Most flow situations of practical interest exhibits an extremely complicated behavior associated to turbulence. The wide range of length and time scales dictates that in most engineering calculations one still has to use Reynolds decomposition, which describes the turbulent motion as a random variation about a mean value. The Reynolds stress tensor  $\overline{u_i u_j}$  that results from this average can be evaluated from its modeled transport equations derived from the Navier-Stokes equations. Nevertheless, this approach, known as second moment closure, has failed to yield for all flow situations better predictions than those returned by simpler closures so as to justify its greater computational cost. Additionally, the near-wall

region where viscous effects are significant cannot be taken into account in second-moment closures with the generality needed in complex flow geometries.

A second route for turbulence modeling is to assume that the diffusive nature of a turbulent flow is analogous to that of a laminar flow and may be represented by a much larger diffusivity. This is the basis of Boussinesq's hypothesis of a 'turbulent' or 'eddy' viscosity  $\nu_t$ , which considers the Reynolds stresses  $\overline{u_i u_j}$  to be proportional to the velocity gradient, in an analogy to viscous stresses, as follows:

$$\overline{u_i u_j} = -\nu_t \left[ \frac{\partial U_i}{\partial x_j} + \frac{\partial U_j}{\partial x_i} \right] + \frac{2}{3} \delta_{ij} k \quad , \quad (1)$$

where  $\delta_{ij}$  is the Kronecker delta and the kinetic energy of the turbulent motion,  $k$ , is defined as  $k = (\overline{u_i u_i})/2$ .

By far the most common choice for calculating of  $\nu_t$  has been that in terms of the turbulence kinetic energy  $k$  and its rate of dissipation,  $\epsilon$ . Launder and Spalding (1974) proposed the first version of such a model that could applied with success to a considerable number of flows. In a subsequent work, Jones and Launder (1972a, 1972b) included low-Reynolds-number effects into the  $k$ - $\epsilon$  model so that it can be used to compute near-wall flows as well as those where wall effects are not present. Later, Launder and Sharma (1974) modified slightly some damping functions in the Jones & Launder's model and today this modified version is probably the most used turbulence closure for engineering calculations. The main reason for the success attained by the  $k$ - $\epsilon$  model can be attributed in part to its robustness, economy and acceptable results in the predictions of several flows. However, the model is known to have deficiencies in flow situations involving streamline curvature, adverse pressure gradient and separated regions.

More recently, Yakhot et al. (1992) offered a new theoretical frame, known as Renormalization Group (RNG) theory, to derive an alternative version of  $k$ - $\epsilon$  model that removes part of the anomalies usually associated to  $k$ - $\epsilon$  models. In the so-called RNG  $k$ - $\epsilon$  model constants and functions are evaluated by the theory and not by empiricism as is the case of other versions. Additionally, the model can be applied to the near-wall region without recourse to wall-functions or ad-hoc function in the transport equations of the turbulence quantities. This mathematical foundation is pointed out by Orszag et. al. (1993) as the main reason why the RNG  $k$ - $\epsilon$  model should have a wider range of applicability, as compared with standard models. A support to this claim is reported by Yakhot et al. (1992) for the case of a turbulent flow over a backward facing step, where the RNG  $k$ - $\epsilon$  model is seen to produce much better results than standard versions of  $k$ - $\epsilon$  models.

Several works have considered the application of the RNG  $k$ - $\epsilon$  model to complex flow situations and some provide a comparison of its performance with other versions of  $k$ - $\epsilon$  model. However, most investigations restrict themselves to exploring results for velocity and pressure. The present work is a further test of the RNG  $k$ - $\epsilon$  model, applied to a flow situation where other  $k$ - $\epsilon$  models failed to reproduce the experimental data. In addition to results of velocity and pressure, comparisons for turbulence quantities are also provided to clarify differences found between different turbulence models adopted in the work. The radial diffuser flow chosen for this comparative analysis is a good test case since it includes regions of stagnation, stiff pressure gradient, separation and streamline curvature.

Figure 1 shows the main parameters of a radial diffuser that affect the flow. Basically, the fluid enters axially the feeding orifice of diameter  $d$  with uniform velocity  $U_{in}$ , hits the front disk of diameter  $D$  with inclination  $\alpha$  and then a radial flow is established. Attempts to solve

the flow through the diffuser with parallel disks using standard versions of  $k$ - $\epsilon$  models did not capture the pressure distribution on the front disk surface available from experiments (Deschamps et al., 1988, Deschamps et al., 1989). The lack of agreement with experimental data was attributed to the incorrect prediction of separated flow regions at the entrance of the diffuser. Recently, the RNG  $k$ - $\epsilon$  model has been successfully applied to the same flow situation (Deschamps et al., 1996) for different Reynolds number,  $Re (=U_{in}d/\nu)$ , diameter ratios,  $D/d$ , and gap between the disks,  $s_c/d$ .

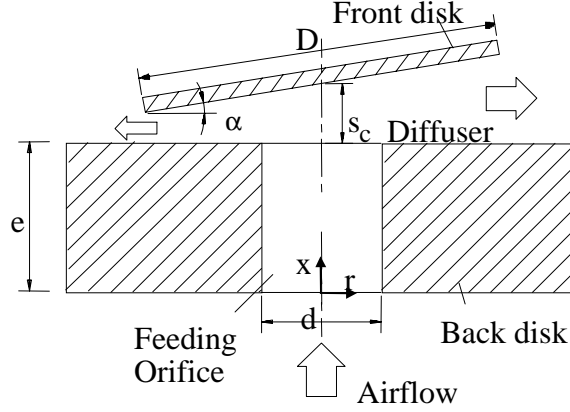


Figure 1: Schematic view of a radial diffuser.

## 2. TURBULENCE MODELS

The transport equations for  $k$  and  $\epsilon$  corresponding to the  $k$ - $\epsilon$  model of Launder & Sharma (1974), denoted here as LS  $k$ - $\epsilon$  model, and to the RNG  $k$ - $\epsilon$  model of Orzag et al. (1993) can be summarized in the form of the following equations:

$$U_j \frac{\partial k}{\partial x_j} = \frac{\partial}{\partial x_j} \left[ \left( \nu + \frac{\nu_t}{\sigma_k} \right) \frac{\partial k}{\partial x_j} \right] + \nu_t S^2 - \epsilon + D \quad (2)$$

$$U_j \frac{\partial \epsilon}{\partial x_j} = \frac{\partial}{\partial x_j} \left[ \left( \nu + \frac{\nu_t}{\sigma_\epsilon} \right) \frac{\partial \epsilon}{\partial x_j} \right] + c_{\epsilon 1} \frac{\epsilon}{k} \nu_t S^2 - c_{\epsilon 2} \frac{\epsilon^2}{k} + E \quad (3)$$

where  $S^2 = 2S_{ij}S_{ij}$  is the modulus of the rate-of-strain tensor. The eddy viscosity appearing in equations (2) and (3) is defined as:

$$\nu_t = c_\mu \frac{k^2}{\epsilon} + M \quad (4)$$

Table 1 summarizes parameters ( $c_\mu$ ,  $c_{\epsilon 1}$  and  $c_{\epsilon 2}$ ) and terms ( $D$ ,  $E$  and  $M$ ) appearing in equations (2)-(4) according to the turbulence model being considered.

The damping functions adopted in  $c_\mu$  and  $c_{\epsilon 1}$  for the LS  $k$ - $\epsilon$  model is necessary to produce a proper diminution of the turbulence structural ratio in the vicinity of a wall. This function is evaluated according to a viscosity dependent parameter,

$$R_t = k^2 / \nu \varepsilon \quad , \quad (5)$$

commonly referred to as turbulence Reynolds number. A first major difference between the models is that in the case of the RNG k- $\varepsilon$  model  $c_\mu$ ,  $c_{\varepsilon 1}$  and  $c_{\varepsilon 2}$  retain their values even in the viscous sub-layer.

Table 1: Parameters and terms in k- $\varepsilon$  models

	LS k- $\varepsilon$ Model	RNG k- $\varepsilon$ Model
$c_\mu$	$0.09 \exp[-3.4 / (1.0 + R_t / 50.0)^2]$	0.0845
$c_{\varepsilon 1}$	$1.44[1.0 - 0.3 \exp(-R_t^2)]$	1.42
$c_{\varepsilon 2}$	1.92	1.68
D	$-2\nu(\partial k^{1/2} / \partial x_i)^2$	0
E	$2\nu v_t (\partial^2 U_i / \partial x_k \partial x_m)^2$	$-c_\mu (\varepsilon^2 / k) \eta^3 (1 - \eta / \eta_0) / (1 + \beta \eta^3)$
M	0	$2k(c_\mu / \varepsilon \nu)^{1/2}$

The term D in the LS k- $\varepsilon$  model had to be included since instead of solving equation (3) for the total dissipation, Jones and Launder (1972a, 1972b) decided to solve it for the isotropic dissipation  $\tilde{\varepsilon}$  defined as

$$\tilde{\varepsilon} = \varepsilon - 2\nu(\partial k / \partial x_j)^2 \quad . \quad (6)$$

This simplifies the wall boundary condition for the dissipation rate  $\tilde{\varepsilon}$ , whose value can be set to zero. The difference between  $\varepsilon$  and  $\tilde{\varepsilon}$  decreases away from the wall, so that in the fully turbulent region they are equivalent. To avoid convergence difficulties, a special treatment is advisable in the implementation of term D of the LS k- $\varepsilon$  model (see Sinha & Candler, 1998).

The main distinction between these two turbulence models is represented by term E. For the LS k- $\varepsilon$  model E was simply chosen by convenience so as to improve the result of turbulence kinetic energy profile near the wall. Yet, in the case of the RNG k- $\varepsilon$  model the term E is related to the rate-of-strain tensor, through the ratio of turbulence to mean strain time scale  $\eta$  defined as

$$\eta = S k / \varepsilon \quad , \quad (7)$$

and has an important role on  $\varepsilon$  level when the strains are large. Constants  $\eta_0$  and  $\beta$  appearing in Table 1 are given values of 4.38 and 0.012, respectively. The term E may change sign depending on whether the time scale ratio  $\eta$  is greater than the value  $\eta_0$  found in homogenous shear flows. In regions of small strain rate, the term E has a trend to increase  $v_t$  somewhat, whereas in regions of elevated strain rate the sign of E becomes positive and  $v_t$  is considerably reduced. This feature of the RNG k- $\varepsilon$  is responsible for substantial improvements verified in the prediction of large separation flow regions.

Finally, the Prandtl numbers  $\sigma_k$  and  $\sigma_\epsilon$  in equations (2) and (3) are equal to 1.0 and 1.3, respectively, for the LS k- $\epsilon$  model but assume a single value for the RNG k- $\epsilon$  model, which is expressed through the inverse of the Prandtl number,  $\gamma (=1/\sigma)$ :

$$\left| \frac{\gamma - 1.3929}{\gamma_0 - 1.3929} \right|^{0.6321} \left| \frac{\gamma + 2.3929}{\gamma_0 + 2.3929} \right|^{0.3679} = \frac{v}{v_{\text{eff}}} \quad (8)$$

with  $\gamma_0 = 1.0$ .

### 3. NUMERICAL METHODOLOGY

A finite volume methodology was employed to integrate the governing differential equations using a non-staggered grid scheme. Interpolation of unknown quantities at the control volume faces were obtained using the QUICK interpolation scheme, which is considered to be a second order procedure. However, for the equations of turbulence quantities the Power Law Differencing Scheme (PLDS) was adopted since the unboundedness of the QUICK scheme usually introduces serious numerical instabilities, causing calculations to diverge. A segregate approach was employed to solve the equations and coupling between pressure and velocity was handled through the SIMPLEC algorithm. The system of algebraic equations that result from the integration of the equations over each control volume is solved using the Tridiagonal Matrix Algorithm (TDMA). Underrelaxation of the iterative procedure was required to avoid divergence during the marching procedure towards convergence. Further details on the numerical methodology can be found in Versteeg & Malalasekera (1995).

Boundary conditions for the governing equations are required at inlet, outlet, walls and locations of symmetry. At the walls, the condition of no-slip and impermeable wall boundary condition were imposed; this implies that  $k = 0$ . For the turbulence dissipation  $\epsilon$ , a value equal to zero could also be adopted at the walls in the case of the LS k- $\epsilon$  model. Yet, for the RNG k- $\epsilon$  model a value was set for the control volumes adjacent to the wall, following a non-equilibrium wall-function. In the symmetry locations the normal velocity and the normal gradients of all other quantities were set to zero.

The velocity component normal to the inlet boundary was specified as  $U = U_{\text{in}}$ , with the other components set to zero. Salinas Casanova (2000) has shown that this uniform velocity condition is adequate since the inflow velocity profile at the feeding orifice plays no significant role in the solution of the flow field in the diffuser. Numerical tests revealed that when the turbulence intensity  $I$  varied from 3% to 6% no significant was observed in the predicted flow. Therefore, a value of 3% was adopted in the calculation of all results shown in this work. The dissipation rate at the inlet was estimated based on the assumption of equilibrium boundary layer, that is  $\epsilon = (c_\mu k^2)^{3/4} / \ell_m$ , with  $c_\mu = 0.09$  and the mixing length  $\ell_m = 0.07 d/2$ .

At the outlet boundary the solution domain was extended well beyond the diffuser exit, so that the atmospheric pressure verified in the experiment could be set to the outlet. The boundary condition for  $k$  in this case was fixed according to a turbulence intensity of 3% whereas the dissipation rate was estimated based on the same assumption of equilibrium boundary layer used at the inlet. Given the wall jet characteristic of the flow exiting the diffuser it is expected that any inaccuracy of the above outlet condition will not have a significant impact on the numerical solution.

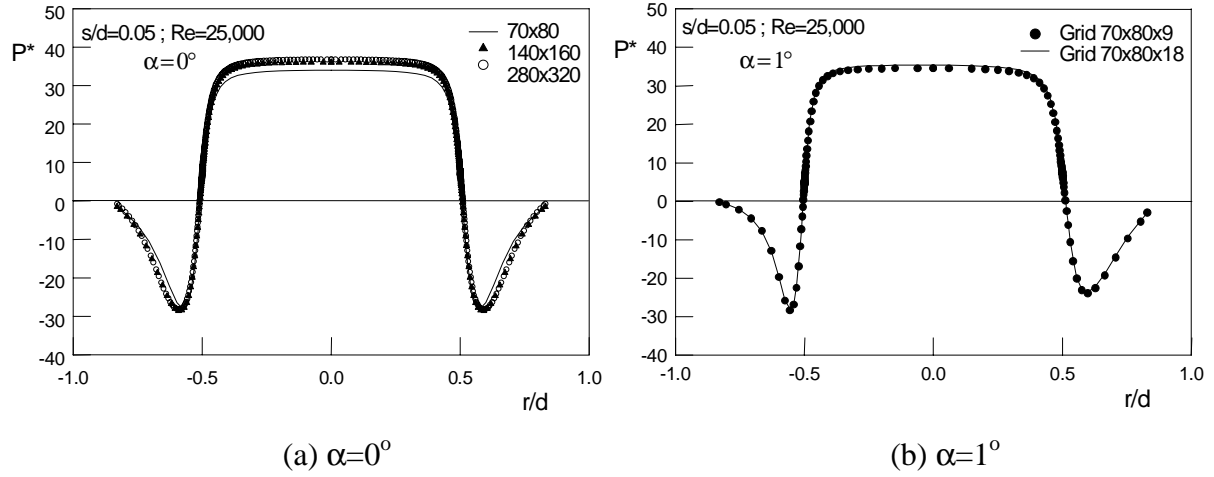
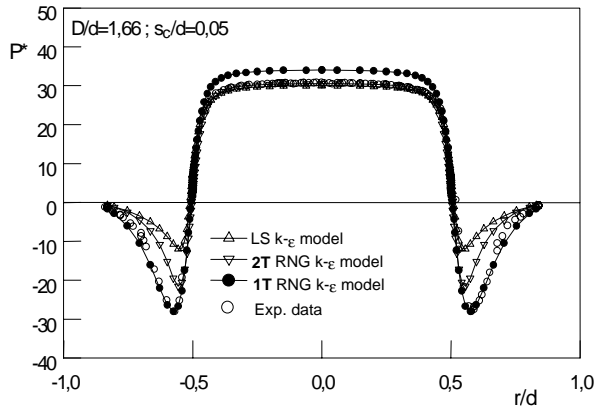


Figure 2: Sensitivity of results for pressure distribution to mesh refinement;  $D/d=1.66$ .

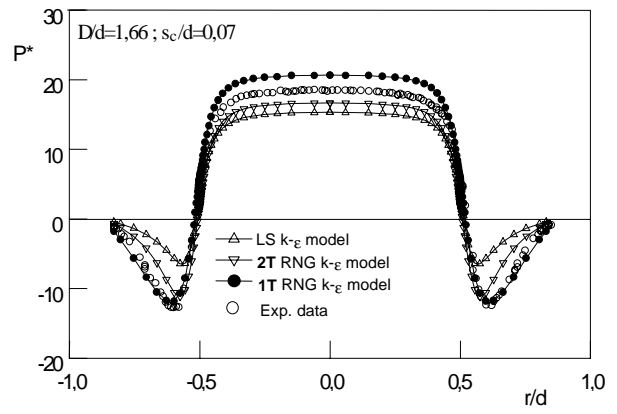
#### 4. RESULTS

A first step in the analysis was to reduce the truncation error in the calculations to a minimum so that the numerical solution could be assumed to represent predictions through the turbulence models. Figure 2 shows typical results of sensitivity tests with respect to the grid refinement for dimensionless pressure  $P^*$  ( $= 2p/\rho U^2$ ) distribution on the front disk surface, considering  $D/d=1.66$ ,  $s_c/d=0.05$ ,  $Re=25,000$  and two different front disk inclinations ( $\alpha= 0^\circ$  and  $1^\circ$ ). Initially a condition of parallel disks was considered since for this two-dimensional flow situation the grid refinement in the axial ( $x$ ) and radial ( $r$ ) directions could be explored to a greater extent. The results yielded by three grid levels (70x80, 140x160 and 280x320, axial x radial) plotted in Fig. 2a show that the less refined grid returns some truncation error. Nevertheless, it was decided that the difference between the results was not such so as to justify the much more expensive computation associated to the more refined grids. For the circumferential direction ( $\theta$ ) the investigation revealed virtually no effect on the pressure distribution when the grid is doubled in that direction, as can be seen from Fig. 2b. Therefore, for the remaining calculations a grid level of 70x80x9 ( $x$ ,  $r$  and  $\theta$ , respectively) was adopted.

Having investigated the level of truncation error in the numerical result the analysis was directed to the performance assessment of each turbulence model for two diameter ratios  $D/d$  ( $= 1.66$  and  $3.0$ ), two gaps  $s_c/d$  ( $= 0.05$  and  $0.07$ ) and three inclinations  $\alpha$  ( $= 0, 1$  and  $2^\circ$ ). All cases considered a Reynolds number  $Re = 25,000$ . Figures 3-5 show the radial pressure distribution along the front disk surface obtained from the experiments and computations with each turbulence models. Details on the experimental setup and procedure will be not given here due to space limitation but can be found elsewhere (Salinas Casanova et al., 1999). There has been some conflicting information in the literature concerning the proper definition for  $v_t$  in the RNG k- $\epsilon$  model. For instance, Orzag et al. (1993) define  $v_t$  according to equation (4) and term  $M$  as defined in Table 1. However, Yakhot et al. (1992) neglect  $M$  in deriving term  $E$ , which is arguably the major benefit, from the turbulence modeling point of view, offered by the RNG k- $\epsilon$  model. Here, it has been decided to use the RNG k- $\epsilon$  model with and without term  $M$  in equation (4); these two versions of the model will be referred hereafter as **2T** RNG k- $\epsilon$  model and **1T** RNG k- $\epsilon$  model, respectively.

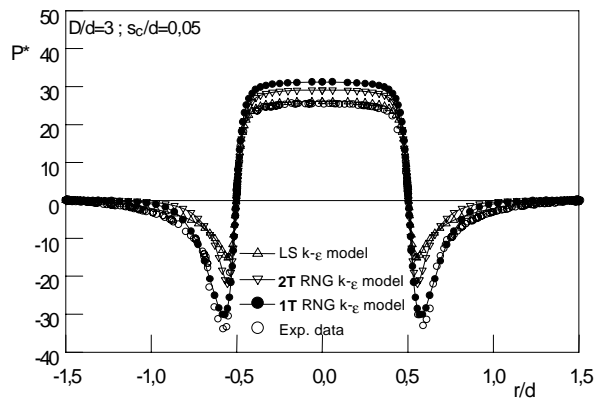


(a)  $s_c/d=0.05$

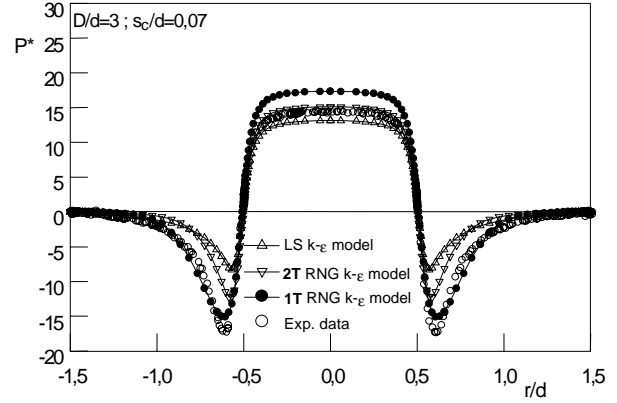


(b)  $s_c/d=0.07$ .

Figure 3: Pressure distribution on the front disk surface:  $D/d=1.66$ ;  $\alpha=0^\circ$ ;  $Re=25,000$ .

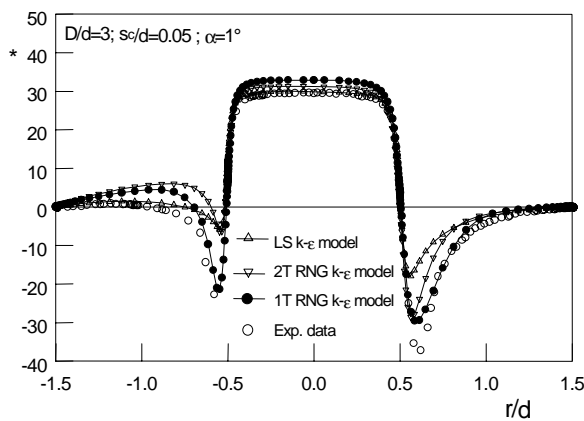


(a)  $s_c/d=0.05$

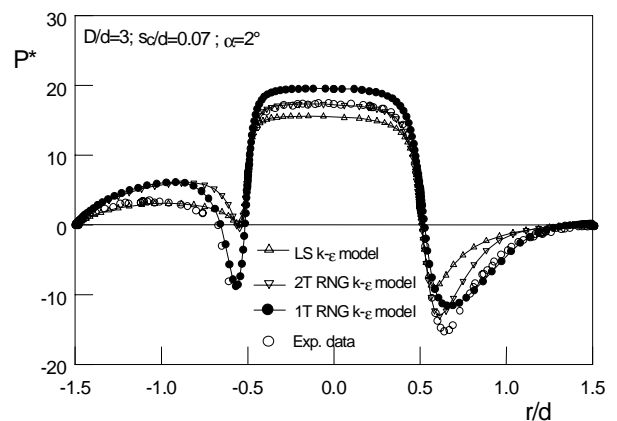


(b)  $s_c/d=0.07$ .

Figure 4: Pressure distribution on the front disk surface:  $D/d=3.0$ ;  $\alpha=0^\circ$ ;  $Re=25,000$ ;



(a)  $s_c/d=0.05$



(b)  $s_c/d=0.07$ .

Figure 5: Pressure distribution on the front disk surface:  $D/d=3.0$ ;  $Re=25,000$ ;

As can be seen from all figures, the presence of the front disk creates a plateau on the central part of the pressure distribution ( $r/d < 0.5$ ). The sharp pressure drop at the radial position  $r/d \approx 0.5$  is associated to the change in the flow direction and to the reduction of the flow passage area. The latter is particularly strong in the range of disk displacement and Reynolds number considered here since, as will be shown shortly, a separated flow region is always present on the back disk at the diffuser entrance. The additional reduction in the passage area originated by this separation results in a further pressure drop due to the increase of local velocity. After reaching its minimum the pressure distribution progresses towards the atmospheric condition at the exit of the diffuser, although in some cases this recovery is not fully accomplished, with the pressure still remaining negative at the diffuser exit.

The agreement between numerical and experimental results in Figs. 3-5 is very poor as far as the LS  $k$ - $\epsilon$  model is concerned, especially at  $r/d \approx 0.5$ , where the pressure drop occurs. On the other hand, predictions given by both versions of the RNG  $k$ - $\epsilon$  model (with and without term  $M$  in the equation for  $\nu_t$ ) are closer to the experimental data. Particularly, when term  $M$  is neglected a markedly improvement in the prediction is verified at  $r/d \approx 0.5$ , although some degradation is visible in the pressure plateau region ( $r/d < 0.5$ ).

In order to understand the physical mechanism behind the level of agreement verified for each turbulence model, Figs. 6-8 were prepared. There, contours for stream function  $\psi$ , dimensionless eddy viscosity  $\nu_t/\nu$  and turbulence length scale  $\ell$  ( $=k^{3/2}/\epsilon$ ) at the diffuser entrance are plotted for  $D/d = 3.0$ ,  $s_c/d = 0.05$ ,  $Re = 25,000$  and  $\alpha = 0^\circ$ . As pointed out before, the pressure drop at  $r/d \approx 0.5$  is associated to the velocity level at the diffuser entrance, which is affected by the presence of any separated flow region there. Therefore, the greater pressure drop observed for the **1T** RNG  $k$ - $\epsilon$  model should be an outcome of its capability to predict a larger separated flow region; Fig. 6c shows that this is precisely the case.

An effective way to diminish or even prevent the flow from separating is through the increase of turbulence level in the region of interest. Figure 7 shows that levels of eddy viscosity predicted by the LS  $k$ - $\epsilon$  model are much higher than those observed for both versions of the RNG  $k$ - $\epsilon$  model. As a consequence, the LS  $k$ - $\epsilon$  model predicts virtually no separation region (Fig. 6a). Naturally, it is difficult to conclude whether such turbulence levels are physically consistent by simply examining results of eddy viscosity. A more convenient choice for this assessment is the evaluation of turbulence length scales. Figure 8a shows that length scales obtained by the LS  $k$ - $\epsilon$  model exceed even the physical dimension left by the gap between the disks ( $s_c/d = 0.05$ ) and suggests therefore an overprediction of turbulence at the diffuser entrance. As expected, both versions of the RNG  $k$ - $\epsilon$  model yield much lower values for length scale (Figs. 8b and 8c).

## 5. CONCLUSIONS

The present work has presented a comparative analysis of the RNG  $k$ - $\epsilon$  model and the Launder & Sharma (LS)  $k$ - $\epsilon$  model. A radial diffuser flow geometry was chosen as the test case since it brings about a number of flow features that make this class of flow difficult to predict. The flow was analyzed for different parameters such as diameter ratios, gap between the disks and inclination of the front disk.

The RNG  $k$ - $\epsilon$  turbulence model was found to reproduce experimental results of pressure distribution on the front disk surface in much better agreement than the LS  $k$ - $\epsilon$  model. The poor performance of the LS  $k$ - $\epsilon$  model had already been verified for the flow through radial diffuser with disks parallel and is also found here when the front disk is inclined. The poor results yielded by the LS  $k$ - $\epsilon$  model is associated to its overpredicted levels of turbulence at the diffuser entrance. The RNG  $k$ - $\epsilon$  model provides much lower levels of turbulence and, as a

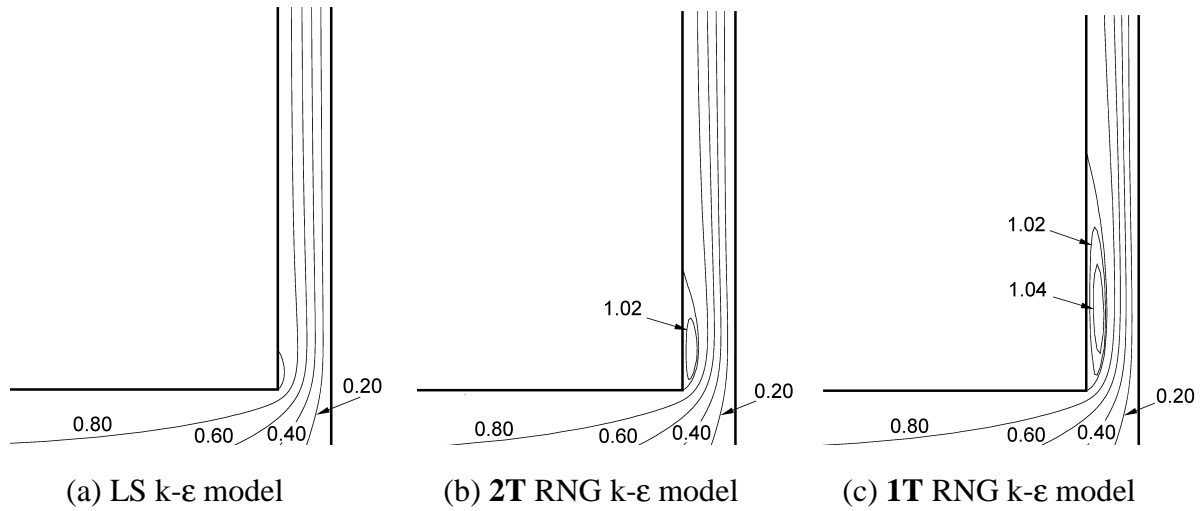


Figure 6: Stream-function contours:  $D/d=3.0$ ;  $s/d=0.05$ ,  $\alpha=0^\circ$  and  $Re=25,000$ .

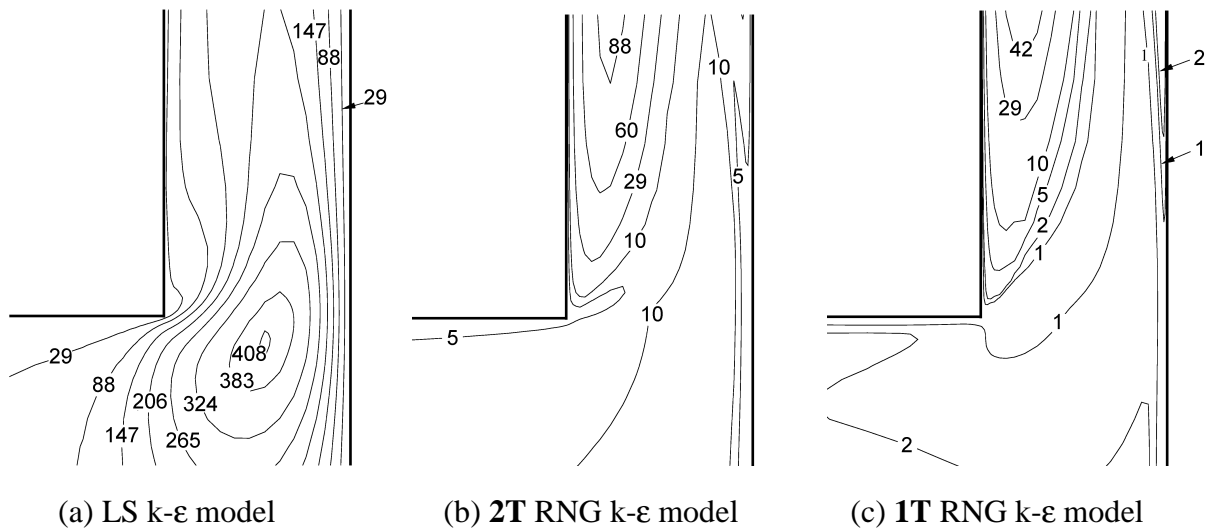


Figure 7: Eddy-viscosity contours:  $D/d=3.0$ ;  $s/d=0.05$ ,  $\alpha=0^\circ$  and  $Re=25,000$ .

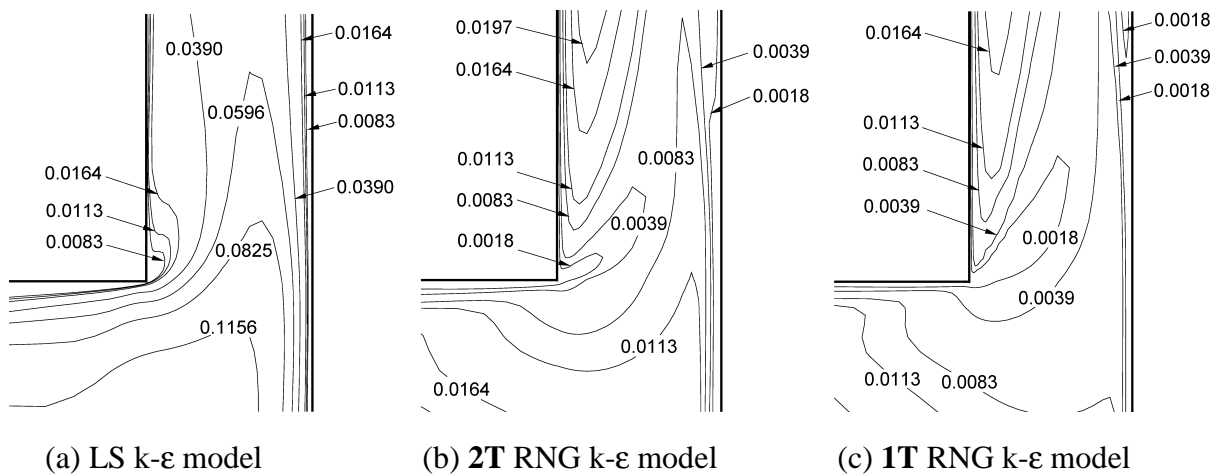


Figure 8: Turbulence length scale contours:  $D/d=3.0$ ;  $s/d=0.05$ ,  $\alpha=0^\circ$  and  $Re=25,000$ .

consequence, captures a separated flow regions as suggested by measurements. A full assessment of the RNG k- $\epsilon$  model regarding its results for turbulence quantities is not possible however, since there is no available experimental data for such quantities.

## REFERENCES

- Deschamps, C. J., Ferreira, R. T. S & Prata, A. T. 1988, "Application of the k- $\epsilon$  Model to Turbulent Flow in Compressor Valves", Proc. 2nd Brazilian Thermal Science Meeting, São Paulo, pp. 259-262 (in Portuguese).
- Deschamps, C. J., Prata, A. T. & Ferreira, R. T. S., 1989, "Turbulent Flow Modeling in Presence of Stagnation, Recirculation, Acceleration and Adverse Pressure Gradient", Proc. X Brazilian Congress of Mechanical Engineering, Rio de Janeiro, Vol. I, pp. 57-60 (in Portuguese).
- Deschamps, C. J., Prata, A. T. & Ferreira, R. T. S., 1996, "Turbulent Flow through Reed Type Valves of Reciprocating Compressors", Proceedings of the 1996 ASME International Congress and Exposition - Symposium on the Analysis and Applications of Heat Pump & Refrigeration Systems, pp. 151-161, Texas, USA.
- Jones, W. P. & Launder, B. E., 1972a, "Some Properties of Sink Flow Turbulent Boundary-Layers", J. Fluid Mech., vol. 56, p. 337-351.
- Jones, W. P. & Launder, B.E., 1972b, "The Prediction of Laminarization with a Two-Equation Model of Turbulence", Int. J. Heat Mass Transfer, vol. 15, p. 301.
- Launder, B. E. & Sharma, B. I., 1974, "Application of the Energy-Dissipation Model of Turbulence to the Calculation of Flow Near a Spinning Disc", Lett. Heat Mass Transfer, Vol. 1, p. 131.
- Launder, B. E., & Spalding, D. B., 1974, "The Numerical Computation of Turbulent Flows", Comp. Meths. Appl. Mech. Engng., vol. 3, pp. 269-289.
- Orzag, S. A., Yakhot, V. Flannery, W. S., Boysan, F., Choudhury, D. Marusewski, J. & Patel, B., 1993, "Renormalization Group Modeling and Turbulence Simulations", So, R. M. C., Speziale, C. G. & Launder, B. E. (eds.), Near-wall turbulent flows. Elsevier Science Publisher.
- Salinas Casanova. D.A., Deschamps, C.J. & Prata, A.T., 1999, "Turbulent Flow through Inclined Valve Reeds", Proc. IMECHE International Conference on Compressor and their Systems, London, UK, pp. 443-452.
- Salinas Casanova. D.A., 2000, "Numerical Analysis of Turbulent Flow through Automatic Valves of Compressors", Ph.D. Thesis, Federal University of Santa Catarina, Brazil (in preparation).
- Sinha, K. & Candler, G. V. 1998, "Convergence Improvement of Two-Equation Turbulence Model Calculations", 29<sup>th</sup> AIAA Fluid Dynamics Conference, A98-32832, Albuquerque, USA.
- Versteeg, H. K. & Malalasekera, W., 1995, "An Introduction to Computational Fluid Dynamics", Longman Scientific & Technical.
- Yakhot, V., Orzag, S. A., Thangam, S., Gtaski, T. B. & Speziale, C. G., 1992, "Development of turbulence models for shear flows by a double expansion technique", Phys. Fluids A, v. 7, pp. 1510-1520.